

Supplementary Information for “Efficient evaluation of quantum observables using entangled measurements”

Appendix A: Pauli graph and LDFC algorithm

In this section, we explain a previous method called grouping with TPB in the main text. The grouping algorithm consists of two parts: the construction of the Pauli graph and its coloring algorithm called the largest-degree-first coloring. These algorithms were implemented in Qiskit^{S1}.

The Pauli graph represents the noncommutativity of the Pauli strings. Its nodes correspond to Pauli strings, and its edges exist if and only if two nodes are *not* qubit-wise commutative. See Algorithm 1 for the algorithm that constructs the Pauli graph using TPB.

Algorithm 1 Construction of Pauli graph

```

1: Input: observable  $A = \sum_{i=1}^n a_i P_i$ . Note that each Pauli string  $P_i$  has length  $N$ .
2: Initialize a graph  $G$  with nodes  $V = \{v_1, \dots, v_n\}$  where  $v_i$  corresponds to Pauli string  $P_i$ .
3: for  $i = 1, \dots, n-1$  do
4:   for  $j = i+1, \dots, n$  do
5:     if any pair of the Pauli operators of Pauli strings  $P_i$  and  $P_j$  are noncommutative then
6:       Span an edge between  $v_i$  and  $v_j$ .
7:     end if
8:   end for
9: end for
10: Return graph  $G$ .
```

After the construction of the Pauli graph, we label the nodes with a rule that neighboring nodes have different labels. The label is called *color*. Since the coloring problem is hard to compute in general, we use a heuristic algorithm, i.e., the largest-degree-first coloring. See Algorithm 2 for details.

Algorithm 2 Largest-degree-first coloring algorithm

```

1: Input: graph  $G = (V, E)$ .
2: Sort the nodes in the descending order of degree on  $G$  and let  $I = \{h_1, \dots, h_n\}$  be the list of node indices. Note that  $v_{h_1}$  has the largest degree.
3: Initialize a list of colors  $C = \{c_1, \dots, c_n\}$ . A color  $c_i$  of  $v_i$  is represented by a non-negative integer number where 0 means that the color has not been assigned yet. All colors are set to be 0 in the initialization.
4: for  $i = 1, \dots, n$  do
5:   Assign the minimum positive integer number to  $c_{h_i}$  that is not equal to the color of any neighbor of  $v_{h_i}$ .
6: end for
7: Return the list of colors  $C$ .
```

Appendix B: Examples of entangled measurements

The first example of entangled measurements, Bell measurements, is shown in the Method section of the main text. The second example of entangled measurements is an omega measurement that is a projective measurement on omega states introduced in the board game Entanglion developed by IBM Research^{S2}. Omega states are defined as follows:

$$|\Omega_0^{YY}\rangle = \frac{1}{2}|00\rangle + \frac{1}{2}|01\rangle - \frac{1}{2}|10\rangle + \frac{1}{2}|11\rangle, \quad (S1)$$

$$|\Omega_1^{YY}\rangle = -\frac{1}{2}|00\rangle + \frac{1}{2}|01\rangle + \frac{1}{2}|10\rangle + \frac{1}{2}|11\rangle, \quad (S2)$$

$$|\Omega_2^{YY}\rangle = \frac{1}{2}|00\rangle + \frac{1}{2}|01\rangle + \frac{1}{2}|10\rangle - \frac{1}{2}|11\rangle, \quad (S3)$$

$$|\Omega_3^{YY}\rangle = \frac{1}{2}|00\rangle - \frac{1}{2}|01\rangle + \frac{1}{2}|10\rangle + \frac{1}{2}|11\rangle. \quad (S4)$$

Herein, we note that omega states are described as omega-YY states because other omega states that can be introduced subsequently. The expectation values of $\sigma^y \otimes \sigma^y$, $\sigma^x \otimes \sigma^z$, and $\sigma^z \otimes \sigma^x$ can be obtained from an omega-YY measurement since the following identities hold:

$$\sigma^y \otimes \sigma^y = |\Omega_1^{YY}\rangle \langle \Omega_1^{YY}| + |\Omega_2^{YY}\rangle \langle \Omega_2^{YY}| - |\Omega_0^{YY}\rangle \langle \Omega_0^{YY}| - |\Omega_3^{YY}\rangle \langle \Omega_3^{YY}|, \quad (S5)$$

$$\sigma^x \otimes \sigma^z = |\Omega_2^{YY}\rangle \langle \Omega_2^{YY}| + |\Omega_3^{YY}\rangle \langle \Omega_3^{YY}| - |\Omega_0^{YY}\rangle \langle \Omega_0^{YY}| - |\Omega_1^{YY}\rangle \langle \Omega_1^{YY}|, \quad (S6)$$

$$\sigma^z \otimes \sigma^x = |\Omega_0^{YY}\rangle \langle \Omega_0^{YY}| + |\Omega_2^{YY}\rangle \langle \Omega_2^{YY}| - |\Omega_1^{YY}\rangle \langle \Omega_1^{YY}| - |\Omega_3^{YY}\rangle \langle \Omega_3^{YY}|. \quad (S7)$$

Circuit implementation of an omega-YY measurement is shown in Fig. S1.

The third and fourth examples are an omega-ZZ measurement and an omega-XX measurement that are projective measurements on the following states:

$$|\Omega_0^{ZZ}\rangle = \frac{1}{\sqrt{2}} |01\rangle - i \frac{1}{\sqrt{2}} |10\rangle, \quad (S8)$$

$$|\Omega_1^{ZZ}\rangle = \frac{1}{\sqrt{2}} |01\rangle + i \frac{1}{\sqrt{2}} |10\rangle, \quad (S9)$$

$$|\Omega_2^{ZZ}\rangle = \frac{1}{\sqrt{2}} |00\rangle - i \frac{1}{\sqrt{2}} |11\rangle, \quad (S10)$$

$$|\Omega_3^{ZZ}\rangle = \frac{1}{\sqrt{2}} |00\rangle + i \frac{1}{\sqrt{2}} |11\rangle, \quad (S11)$$

and

$$|\Omega_0^{XX}\rangle = \frac{1}{2} |00\rangle - \frac{i}{2} |01\rangle + \frac{i}{2} |10\rangle - \frac{1}{2} |11\rangle, \quad (S12)$$

$$|\Omega_1^{XX}\rangle = -\frac{1}{2} |00\rangle - \frac{i}{2} |01\rangle - \frac{i}{2} |10\rangle - \frac{1}{2} |11\rangle, \quad (S13)$$

$$|\Omega_2^{XX}\rangle = \frac{1}{2} |00\rangle - \frac{i}{2} |01\rangle - \frac{i}{2} |10\rangle + \frac{1}{2} |11\rangle, \quad (S14)$$

$$|\Omega_3^{XX}\rangle = \frac{1}{2} |00\rangle + \frac{i}{2} |01\rangle - \frac{i}{2} |10\rangle - \frac{1}{2} |11\rangle. \quad (S15)$$

In the same way as a Bell measurement and an omega-YY measurement, the following two states allow joint measurements of the two-qubit operators. An omega-ZZ measurement is a joint measurement of observables $\sigma^z \otimes \sigma^z$, $\sigma^x \otimes \sigma^x$, and $\sigma^y \otimes \sigma^x$. It can be derived from the following identities:

$$\sigma^z \otimes \sigma^z = |\Omega_2^{ZZ}\rangle \langle \Omega_2^{ZZ}| + |\Omega_3^{ZZ}\rangle \langle \Omega_3^{ZZ}| - |\Omega_0^{ZZ}\rangle \langle \Omega_0^{ZZ}| - |\Omega_1^{ZZ}\rangle \langle \Omega_1^{ZZ}|, \quad (S16)$$

$$\sigma^x \otimes \sigma^y = |\Omega_0^{ZZ}\rangle \langle \Omega_0^{ZZ}| + |\Omega_3^{ZZ}\rangle \langle \Omega_3^{ZZ}| - |\Omega_1^{ZZ}\rangle \langle \Omega_1^{ZZ}| - |\Omega_2^{ZZ}\rangle \langle \Omega_2^{ZZ}|, \quad (S17)$$

$$\sigma^y \otimes \sigma^x = |\Omega_1^{ZZ}\rangle \langle \Omega_1^{ZZ}| + |\Omega_3^{ZZ}\rangle \langle \Omega_3^{ZZ}| - |\Omega_0^{ZZ}\rangle \langle \Omega_0^{ZZ}| - |\Omega_2^{ZZ}\rangle \langle \Omega_2^{ZZ}|. \quad (S18)$$

An omega-XX measurement is a joint measurement of observables $\sigma^x \otimes \sigma^x$, $\sigma^y \otimes \sigma^z$, and $\sigma^z \otimes \sigma^y$. It can be derived from the following identities:

$$\sigma^x \otimes \sigma^x = |\Omega_1^{XX}\rangle \langle \Omega_1^{XX}| + |\Omega_2^{XX}\rangle \langle \Omega_2^{XX}| - |\Omega_0^{XX}\rangle \langle \Omega_0^{XX}| - |\Omega_3^{XX}\rangle \langle \Omega_3^{XX}|, \quad (S19)$$

$$\sigma^y \otimes \sigma^z = |\Omega_0^{XX}\rangle \langle \Omega_0^{XX}| + |\Omega_1^{XX}\rangle \langle \Omega_1^{XX}| - |\Omega_2^{XX}\rangle \langle \Omega_2^{XX}| - |\Omega_3^{XX}\rangle \langle \Omega_3^{XX}|, \quad (S20)$$

$$\sigma^z \otimes \sigma^y = |\Omega_1^{XX}\rangle \langle \Omega_1^{XX}| + |\Omega_3^{XX}\rangle \langle \Omega_3^{XX}| - |\Omega_0^{XX}\rangle \langle \Omega_0^{XX}| - |\Omega_2^{XX}\rangle \langle \Omega_2^{XX}|. \quad (S21)$$

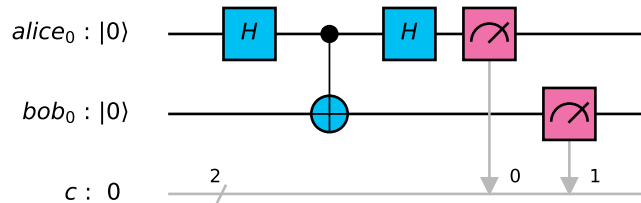


FIG. S1: Quantum circuit of an omega-YY measurement.

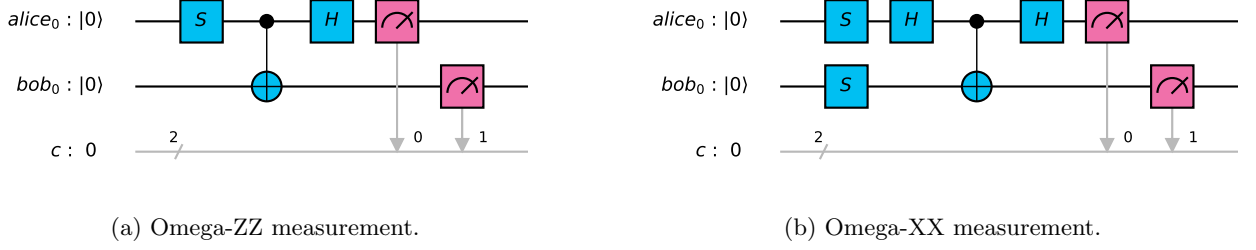


FIG. S2: Quantum circuits of omega-ZZ and omega-XX measurements.

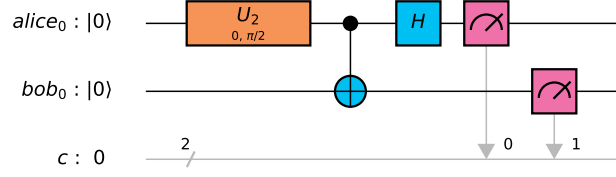


FIG. S3: Quantum circuit of a chi measurement.

Circuit implementations of an omega-ZZ measurement and an omega-XX measurement are shown in Fig. S2.

The fifth example is a chi measurement. A chi measurement is a joint measurement of $\sigma^x \otimes \sigma^y$, $\sigma^y \otimes \sigma^z$, and $\sigma^z \otimes \sigma^x$. Let us define the following states:

$$|X_0\rangle = \frac{1}{2} |00\rangle + \frac{1}{2} |01\rangle + \frac{i}{2} |10\rangle - \frac{i}{2} |11\rangle, \quad (\text{S22})$$

$$|X_1\rangle = \frac{1}{2} |00\rangle + \frac{1}{2} |01\rangle - \frac{i}{2} |10\rangle + \frac{i}{2} |11\rangle, \quad (\text{S23})$$

$$|X_2\rangle = \frac{1}{2} |00\rangle - \frac{1}{2} |01\rangle + \frac{i}{2} |10\rangle + \frac{i}{2} |11\rangle, \quad (\text{S24})$$

$$|X_3\rangle = -\frac{1}{2} |00\rangle + \frac{1}{2} |01\rangle + \frac{i}{2} |10\rangle + \frac{i}{2} |11\rangle. \quad (\text{S25})$$

A chi measurement is a projective measurement of these states as the following identities hold:

$$\sigma^x \otimes \sigma^y = -|X_0\rangle\langle X_0| + |X_1\rangle\langle X_1| + |X_2\rangle\langle X_2| - |X_3\rangle\langle X_3|, \quad (\text{S26})$$

$$\sigma^y \otimes \sigma^z = |X_0\rangle\langle X_0| - |X_1\rangle\langle X_1| + |X_2\rangle\langle X_2| - |X_3\rangle\langle X_3|, \quad (\text{S27})$$

$$\sigma^z \otimes \sigma^x = |X_0\rangle\langle X_0| + |X_1\rangle\langle X_1| - |X_2\rangle\langle X_2| - |X_3\rangle\langle X_3|. \quad (\text{S28})$$

The circuit implementation of a chi measurement is shown in Fig. S3. Herein, we use a one-pulse gate U_2 defined in Qiskit Terra^{S1}. U_2 -gate has two parameters ϕ and λ . The matrix representation of U_2 -gate is

$$\frac{1}{\sqrt{2}} \begin{pmatrix} 1 & -e^{i\lambda} \\ e^{i\phi} & e^{i(\phi+\lambda)} \end{pmatrix} \quad (\text{S29})$$

In Fig. S3, the parameters of U_2 -gate can be expressed as $\phi = 0$ and $\lambda = \frac{\pi}{2}$.

There are entangled measurements with three or more qubits for joint measurement of Pauli strings and they can be realized as similar formulations; however, we used only two-qubit entangled measurements in our experiments. This is because large quantum circuits are required for multipartite entangled measurements in general and it seems difficult to execute such circuits on current quantum computers owing to possible errors that may occur.

Appendix C: Error derived from the grouping

1. Theoretical analysis of the covariance effects by grouping

We assume that observables are given by the following weighted sum of Pauli strings:

$$A = \sum_{i=1}^n a_i P_i \quad (\text{S1})$$

where a_i denotes a real number and P_i denotes a Pauli string. In this section, let us consider the standard error derived from the grouping of Pauli strings. Let a grouping divide n Pauli strings into K sets s_1, s_2, \dots, s_K . Then, the equality

$$A = \sum_{k=1}^K \sum_{i \in s_k} a_i P_i, \quad (\text{S2})$$

holds by definition. If the number of samples for group s_k is S_k , the standard error can be expressed as

$$\epsilon_G = \sqrt{\sum_{k=1}^K \frac{\text{Var} [\sum_{i \in s_k} a_i P_i]}{S_k}} \quad (\text{S3})$$

$$= \sqrt{\sum_{k=1}^K \frac{\sum_{(i,j) \in s_k \times s_k} a_i a_j \langle (P_i - \langle P_i \rangle)(P_j - \langle P_j \rangle) \rangle}{S_k}}. \quad (\text{S4})$$

In the case of no-grouping, i.e., $|s_k| = 1$, the standard error can be expressed as

$$\epsilon_{NG} = \sqrt{\frac{1}{S} \sum_{i=1}^n a_i^2 \langle (P_i - \langle P_i \rangle)^2 \rangle}, \quad (\text{S5})$$

where we assume that $S_k = S$ for simplicity using a constant positive integer S . This error does not contain the covariance effects.

We propose that the number of samples in each group is proportional to the size of the group, i.e., $S_k = |s_k|S$, where the total numbers of samples for no-grouping and grouping are the same. Let us compare the standard error without grouping ϵ_{NG} and that with grouping ϵ_G as follows:

$$\epsilon_G^2 = \sum_{k=1}^K \frac{\sum_{(i,j) \in s_k \times s_k} a_i a_j \langle (P_i - \langle P_i \rangle)(P_j - \langle P_j \rangle) \rangle}{S_k} \quad (\text{S6})$$

$$= \frac{1}{S} \sum_{k=1}^K \frac{\sum_{(i,j) \in s_k \times s_k} \langle (a_i P_i - \langle a_i P_i \rangle)(a_j P_j - \langle a_j P_j \rangle) \rangle}{|s_k|} \quad (\text{S7})$$

$$\leq \frac{1}{S} \sum_{k=1}^K \frac{\sum_{(i,j) \in s_k \times s_k} \sqrt{\langle (a_i P_i - \langle a_i P_i \rangle)^2 \rangle \langle (a_j P_j - \langle a_j P_j \rangle)^2 \rangle}}{|s_k|} \quad (\text{S8})$$

$$\leq \frac{1}{S} \sum_{k=1}^K \frac{\sum_{(i,j) \in s_k \times s_k} [\langle (a_i P_i - \langle a_i P_i \rangle)^2 \rangle + \langle (a_j P_j - \langle a_j P_j \rangle)^2 \rangle]}{2|s_k|} \quad (\text{S9})$$

$$= \frac{1}{S} \sum_{k=1}^K \sum_{i \in s_k} \langle (a_i P_i - \langle a_i P_i \rangle)^2 \rangle \quad (\text{S10})$$

$$= \epsilon_{NG}^2, \quad (\text{S11})$$

where we applied the Cauchy–Schwarz inequality to the first inequality (S8) and the AM–GM inequality to the second inequality (S9). As a result, we obtain the following theorem:

Theorem 1. *The standard error of grouping is less or equal to that of no-grouping; i.e., the inequality*

$$\epsilon_G \leq \epsilon_{NG}, \quad (\text{S12})$$

holds.

2. Numerical experiment

Herein, we present the two-qubit antiferromagnetic Heisenberg model, which can be expressed as

$$H = J(\sigma^x \sigma^x + \sigma^y \sigma^y + \sigma^z \sigma^z), \quad (\text{S13})$$

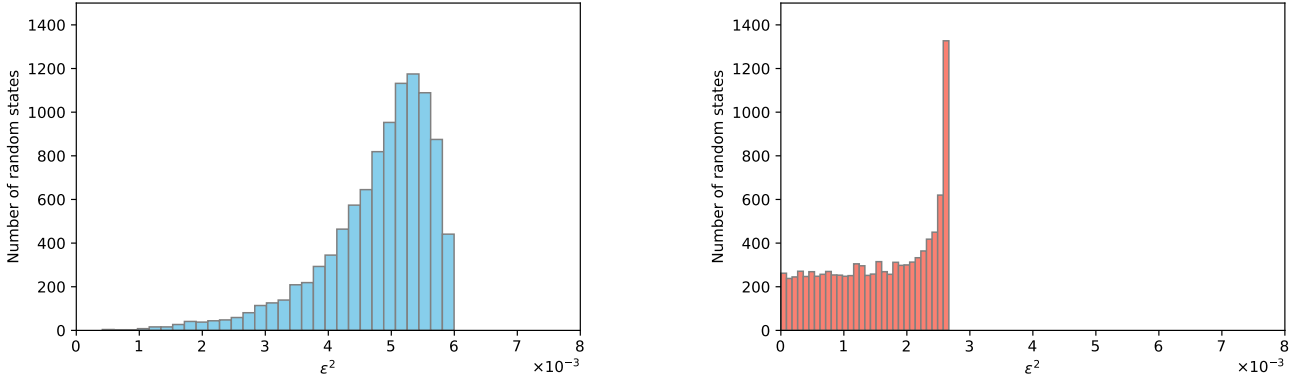
with $J > 0$. We assume $J = 1$ for simplicity. A variance of this Hamiltonian is

$$\text{Var}[H]_{NG} = \text{Var}[\sigma^x \sigma^x] + \text{Var}[\sigma^y \sigma^y] + \text{Var}[\sigma^z \sigma^z], \quad (\text{S14})$$

if one performs measurements $\sigma^x \sigma^x$, $\sigma^y \sigma^y$, and $\sigma^z \sigma^z$ independently. If one performs a joint measurement (Bell measurement), a variance of the Hamiltonian can then be expressed as

$$\begin{aligned} \text{Var}[H]_G &= \text{Var}[\sigma^x \sigma^x + \sigma^y \sigma^y + \sigma^z \sigma^z] \\ &= \text{Var}[\sigma^x \sigma^x] + \text{Var}[\sigma^y \sigma^y] + \text{Var}[\sigma^z \sigma^z] + 2 \text{Cov}[\sigma^x \sigma^x, \sigma^y \sigma^y] + 2 \text{Cov}[\sigma^y \sigma^y, \sigma^z \sigma^z] + 2 \text{Cov}[\sigma^z \sigma^z, \sigma^x \sigma^x]. \end{aligned}$$

We numerically computed the square of the standard errors for Pauli strings and grouped Pauli strings using a Bell measurement. We used 10,000 random states of Haar random unitary to calculate the standard errors. The number of running circuits is 500 samples per Pauli strings for no-grouping (three groups) and 1500 samples per group for a Bell measurement (one group). The average of the squared standard errors of no-grouping is 0.00479 and that of the grouping with a Bell measurement is 0.00159. This numerical result shows that the grouping with Bell measurement has less standard error. See Fig. S4 for the distributions. The distribution for the grouping with a Bell measurement is interesting because the values are concentrated around the upper bound, and this characteristic is not seen in the case of the grouping with TPB (refer to Fig. S5. in the Supplementary Information of Kandala et al.^{S3}). This might be an intrinsic property of the grouping with entangled measurements.



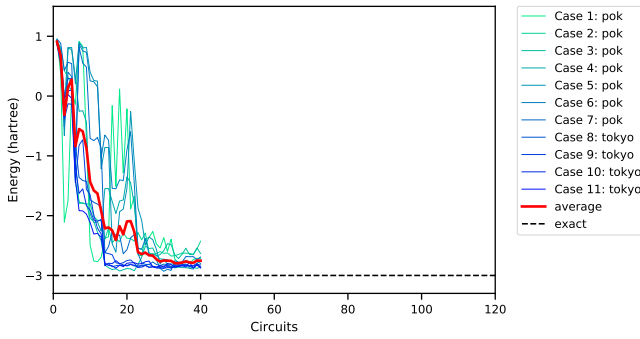
(a) The square of the standard error for Pauli strings (no-grouping) is $\text{Var}[H]_{NG}/500$. We run 500 samples per each of measurements.

(b) The square of the standard error for Pauli strings (grouping by a Bell measurement) is $\text{Var}[H]_G/1500$. We run 1500 samples of the Bell measurement.

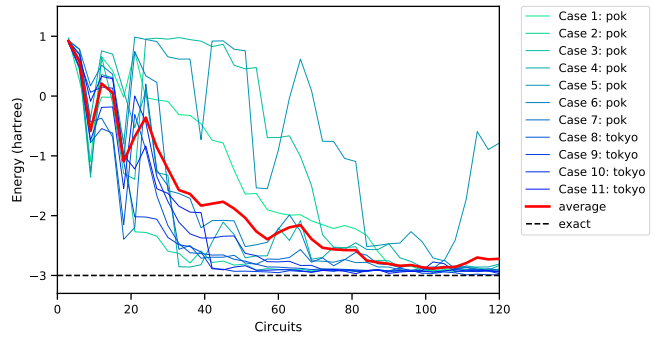
FIG. S4: Comparison of distributions of the square of standard errors. Both values are computed for 10,000 random states. From Theorem 1, the values on the left are greater than those on the right for the same quantum state.

Appendix D: Convergence of VQE on real quantum computers

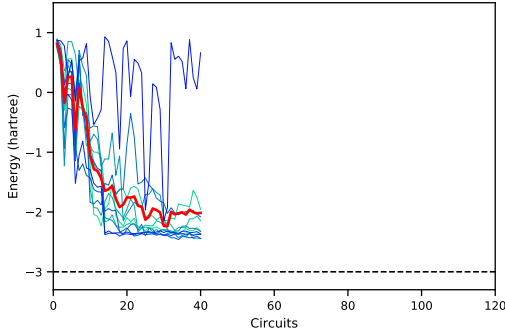
We executed VQE on quantum computers several times (including the result of VQE experiment with entangled measurements of the main text) and plotted the results as shown in Fig. S5. In the experiments on VQE, it took from several minutes to several hours to run a circuit on the quantum computers depending on the waiting time of the job queue. Thus, the experiments took a long time to execute all circuits. The results depend on the device conditions, and the condition may change during the waiting time. Although the energy failed to converge in a few experiments, they converged faster when using the proposed method than when using the baseline in the cases where both methods converged.



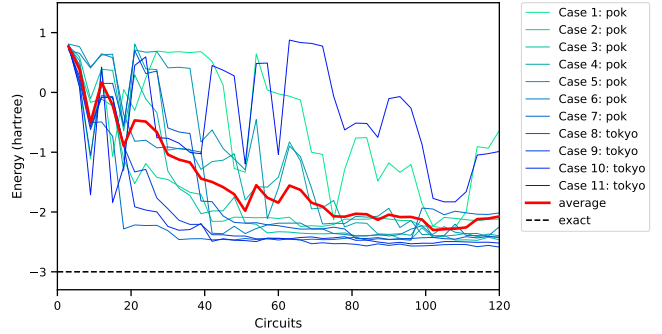
(a) Grouping with Bell measurement with error mitigation.



(b) No-grouping with error mitigation



(c) Grouping with Bell measurement without error mitigation.



(d) No-grouping without error mitigation.

FIG. S5: Experimental results of VQE on quantum computers. In the labels, “pok” and “tokyo” denote that the experiments were conducted on the IBM Q Poughkeepsie and IBM Q Tokyo, respectively. The optimizer SPSA outputs plus and minus values, but we plotted only the mean value of plus and minus values. The label “average” is the average of all cases. These experiments were conducted from June 4 to July 14, 2019.

In some cases, the energy went down once and then went up again. Thus, the converged values are not always the minimum. This implies that SPSA is not robust enough to the noise, and we need to try more optimizers to determine a robust one. We also need to save the states of the optimizer as the checkpoint and go back to the checkpoint if such fluctuation is detected.

REFERENCES

- [S1]Abraham, H. *et al.* Qiskit: An Open-source Framework for Quantum Computing. doi:10.5281/zenodo.2562110 (2019).
- [S2]Entanglion. <https://entanglion.github.io/> (2018). Accessed 29 January 2020.
- [S3]Kandala, A. *et al.* Hardware-efficient variational quantum eigensolver for small molecules and quantum magnets. *Nature* **549**, 242–246 (2017).